End-of-life disposal of libration point orbit spacecraft

Zubin P. Olikara,* Gerard Gómez,† Josep J. Masdemont‡

Abstract

In this work we investigate end-of-life trajectories for spacecraft in orbit about the Sun-Earth L_1 and L_2 libration points. A plan for decommission is often required during the mission design process. We study the spacecraft's natural dynamics in both a high-fidelity model and the circular restricted three-body problem. In particular, we consider the role of the unstable manifold and forbidden regions in determining disposal outcomes. A simple maneuver scheme to prevent returns to the Earth vicinity is also analyzed. We include discussion on potential collision orbit schemes.

1 Introduction

An end-of-life plan is a fundamental aspect of current and future space missions. This is a well-recognized requirement for Earth-orbiting satellites given the need to prevent the accumulation of space debris in these important orbital zones [1]. Libration point orbits are also important regions of interest for current and future missions. The most commonly used libration points, the Sun–Earth L_1 and L_2 points, have an unstable dynamical component, causing spacecraft to naturally depart this regime. These departure trajectories, however, can have many possible outcomes including returns to the Earth vicinity. Thus, consideration should be given to the selection of the desired outcome subject to mission constraints.

The design of libration point trajectories has evolved over the last several decades. The first spacecraft to orbit a libration point was the International Sun–Earth Explorer (ISEE-3) launched in 1978. After its original mission at an L_1 halo orbit and extended mission as a cometary explorer were complete, it was decommissioned into a heliocentric orbit and is due for a passage by the Earth in August 2014 [2]. In 1995 the Solar and Heliospheric Observatory (SOHO) spacecraft, developed by ESA and NASA, became the first to use a trajectory designed using dynamical systems techniques [3]. These techniques, particularly the use of stable and unstable manifolds, will be leveraged in the current study. Example of more recent missions include ESA's HERSCHEL and PLANCK spacecraft launched together in 2009. They were placed into a halo and Lissajous orbit, respectively, about the Sun–Earth L_2 libration point. Their decommissioning was done earlier this year, and it was selected to do the following (update) [4]. Several future libration point missions are planned as well [5].

Constraints present during the decommissioning process are distinguishable from other mission phase requirements. These constraints play a fundamental role in the end-of-life analysis and the determination of feasible trajectories. In the current study, the primary requirements we consider are the following:

- Protection of the Earth and its satellite orbit zones. This is where the Earth-orbiting space debris problem connects with libration point mission design. A spacecraft passing through protected regimes such as the low-Earth or geosynchronous orbits have strict requirements to mitigate the possibility of collisions [1]. Furthermore, if a spacecraft reenters the Earth's atmosphere, a detailed analysis is required to ensure it does so in a safe manner. For a spacecraft using nuclear power generation, strict avoidance of the Earth is necessary.

- Limited fuel remaining aboard the spacecraft. After a spacecraft completes its primary mission, a majority of its fuel will be spent. It is expected, however, that future missions will have some fuel budgeted specifically for the end-of-life phase. In our analysis, we assume that about 100 m/s of Δv to be about the maximum available maneuver capability with potentially less being possible.

- Restricted time window for final maneuvers. Due to mission operating costs, it is desirable for decommissioning to be completed in the least amount of time possible. Ideally, all maneuvers would be completed within 3 to 6 months, though this may not always be feasible. We consider a decommission period of about 1 year to

*Institut d'Estudis Espacials de Catalunya (IEEC) & Universitat de Barcelona (UB), Spain, zubin@maia.ub.es

†IEEC & UB, Spain, gerard@maia.ub.es

‡IEEC & Universitat Politecnica de Catalunya (UPC), Spain, josep@barquins.upc.edu

be about the maximum practical time available.

- Minimal end-of-life complexity. If very careful planning and maneuvering is necessary for a disposal scheme, the associated costs and risks may make it less desirable than a simpler, though perhaps nominally less appealing, option. A robust scheme is preferred to minimize the chance of complications and to maximize the chance of successful disposal.

Individual mission needs will introduce additional constraints to the design process. The aim of this paper, however, is to give an initial analysis of the dynamics and some general disposal options available including associated costs. This work could be viewed as a starting point for a particular mission's end-of-life study.

1.1 Modeling

Since the libration points are features associated with the circular restricted three-body problem (CR3BP), this will be the principal model for the current study. The CR3BP considers the motion of two massive primary bodies (i.e., the Sun and the Earth) that are assumed to move in a circular orbit about their center of mass. Let a third body (i.e., the spacecraft) be positioned at $\mathbf{r} = (x, y, z)$ in a barycentric rotating frame defined such that the primary bodies are fixed along the x-axis. The third body's six-dimensional state $(\mathbf{r}, \mathbf{v})$ is governed by the non-dimensionalized equation of motion

$$\begin{pmatrix} \dot{\mathbf{r}} \\ \dot{\mathbf{v}} \end{pmatrix} = \begin{pmatrix} \mathbf{v} \\ U_{\mathbf{r}} + 2\mathbf{v} \times \hat{\mathbf{z}} \end{pmatrix}, \tag{1}$$

which includes a force potential-like function

$$U(\mathbf{r}) := \frac{1-\mu}{r_1} + \frac{\mu}{r_2} + \frac{1}{2}\left(x^2 + y^2\right).$$

The parameter $\mu \in [0, 0.5]$ relates the primaries' masses, r_1 and r_2 are the distances of the third body to each primary (the larger and smaller primaries are located at $x = -\mu$ and $x = 1-\mu$, respectively), and $\hat{\mathbf{z}}$ is a unit vector along the z-axis, the direction of the system's angular momentum. For the Sun–Earth system, we use mass parameter $\mu = 3.0404234 \times 10^{-6}$.[1] The CR3BP's five equilibrium points are the L_1–L_5 libration points. The L_1 libration point lies between the Sun and the Earth on the x-axis. The L_2 libration point lies beyond the Earth on the x-axis. Additional discussion of the CR3BP can be found in many references including [6].

An important consequence of this model (1) is that it admits an integral of motion. We will use one version of this integral known as the Jacobi constant,[2]

$$C(\mathbf{x}) := 2U(\mathbf{r}) - \|\mathbf{v}\|^2, \tag{2}$$

which is a function of the spacecraft's state. When the equations of motion are derived from a Hamiltonian perspective, an equivalent integral $H \equiv -C/2$ is obtained. This integral serves an energy-like constant, so an increase in the Jacobi constant corresponds to a decrease in the spacecraft's "energy."

We will leverage the existence of an integral of motion to analyze end-of-life trajectories. Fixing a Jacobi constant level C_0 and examining equation (2), we must have $2U(\mathbf{r}) \geq C_0$. Regions in position space where this inequality is violated are referred to as forbidden regions. The boundary satisfies the relation $2U(\mathbf{r}) = C_0$, which requires that $\mathbf{v} = \mathbf{0}$. This so-called zero-velocity surface (ZVS) is a two-dimensional manifold in the three-dimensional position space. If we consider motion restricted to the plane of the primaries, the boundary is a one-dimensional zero-velocity curve (ZVC) that forms a barrier in the two-dimensional position space. We illustrate the ZVC and forbidden region in Figure 1 for three different Jacobi constant levels. In the first illustration, there is a "bottleneck" region around the Earth that allows a spacecraft to access the interior region about the Sun and the exterior region away from the primaries. As the Jacobi constant is increased (i.e., the energy is decreased), the opening at the L_2 libration point closes as shown in the second illustration. As it is further increased, the opening at L_1 closes. These boundaries set access routes to the Earth vicinity and will play a role in the end-of-life design presented.

While the CR3BP captures much of the relevant dynamics, for higher-fidelity end-of-life analysis we use the precise positions of solar system bodies available in NASA Jet Propulsion Laboratory's DE422 ephemeris [7]. In particular, we include the positions of the Sun, Earth, and Moon. We only include their point mass gravitational influence neglecting any non-uniformities in their gravitational field. Additional perturbations such as solar radiation pressure are not incorporated. We arbitrarily select an epoch of 18:00 UTC on January 1, 2015 for this preliminary study. Numerical integration is performed using a Bulirsch–Stoer algorithm [8] with error tolerances of 10^{-12} (or tighter).

[1] This parameter was determined using the combined masses of the Earth and the Moon as the smaller primary's mass.

[2] Some authors include a constant term $\mu(1-\mu)$ in this definition.

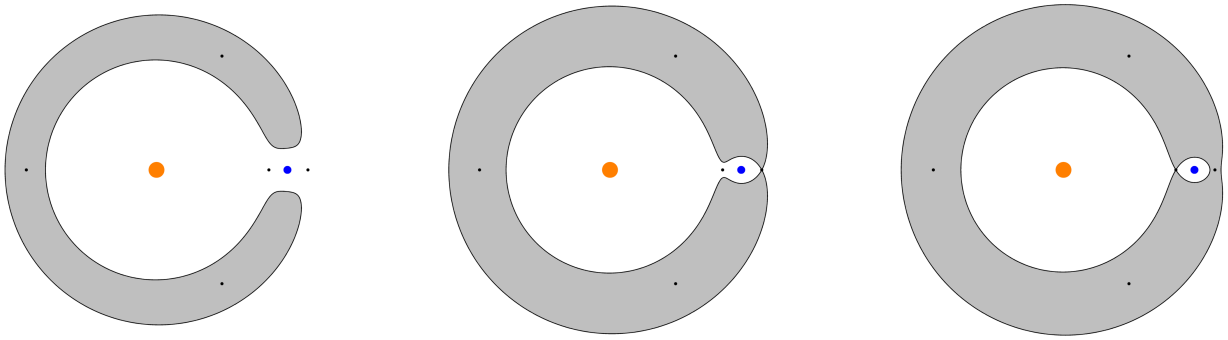

Figure 1: zero-velocity curve (gray region is forbidden) - not to scale for Sun–Earth (*remake with smaller mass parameter)

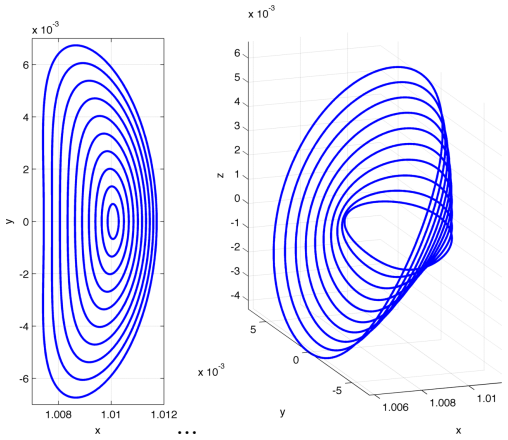

Figure 2: reference L_2 periodic orbits (Lyapunovs and halos)

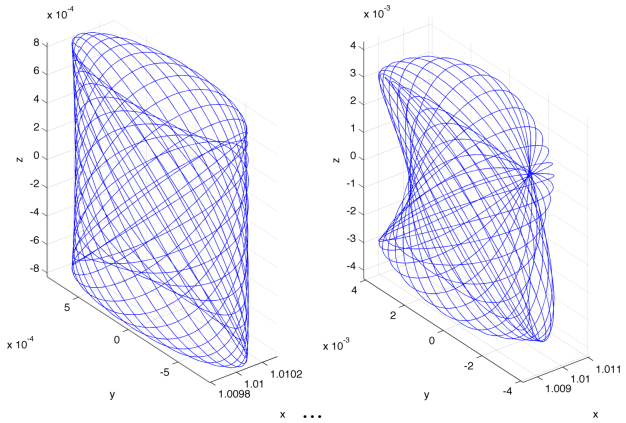

Figure 3: reference L_2 "square" Lissajous orbits

1.2 Reference solutions

The analysis will consider a set of nominal libration point orbits in the Sun–Earth CR3BP that serve as the starting point for the analysis. The L_1 and L_2 libration points have stability of type center × center × saddle. In the plane of the primary bodies, we consider the Lyapunov family of periodic orbits about L_2 shown in Figure 2 with y-amplitude increments of 100,000 km. Note that the plot axes use astronomical units (1 AU = 149,600,000 km). When the family crosses a y-amplitude of approximately 650,000(?–verify) km, it bifurcates into the out-of-plane L_2 halo periodic orbit family. Some members of the "northern" family are shown in Figure 2 with z-amplitude increments of 100,000 km. The "southern" family has an identical structure mirrored across the primaries' plane.

Note that these families of periodic solutions represent just a small part of the libration points center manifold. Nevertheless, they capture much of the relevant motion of nearby quasi-periodic solutions. Thus, for this initial analysis, we will primarily focus on spacecraft originating in a periodic orbit. Given the interest in Lissajous-type trajectories, however, we will also consider the quasi-periodic solutions shown in Figure 3. These "square" Lissajous orbits have approximately equal y- and z-amplitudes, one with amplitudes of 100,000 km and the other with amplitude 600,000 km.

For simplicity and to limit the scope of the current end-of-life analysis, we are focusing on the L_2 families of orbits. The L_1 families appear to exhibit similar trends due to the small mass parameter of the Sun–Earth system. We will note the differences where applicable. For example, an exterior trajectory originating at an L_2 orbit and an interior trajectory originating at an L_1 orbit may revolve around the rotating frame barycenter in opposite directions, but qualitatively they exhibit similar behavior.

1.3 Analysis approach

The paper is organized as follows. We will first consider natural dynamics of a spacecraft originating in a libration point orbit. We will verify that the relevant dynamics are captured by the CR3BP and that the flow away from the initial orbit is dominated by the unstable manifold. In addition, we will discuss the role the ZVS plays in bounding the spacecraft's motion and investigate the associated probabilities of a return to the Earth vicinity. In order to reduce this outcome's probability, we will then consider performing a simple maneuver to modify the ZVS geometry. The cost associated with various maneuver locations will be presented. Discussion will also be made on terminal trajectories that impact a body. Note that during the course of this analysis, we will consider simple impulsive maneuvers. This helps to simplify the analysis, while also reflecting the desire to avoid complex maneuver schemes during the mission decommissioning phase. While other means of thrust, particularly low-thrust schemes, will not be considered, one of the primary drivers of this analysis is the limited fuel remaining during the end-of-life phase. Thus, natural dynamics play a fundamental role and the particular thrust method will be of somewhat lesser importance.

2 Natural dynamics

In this section, we will investigate the natural motions of a spacecraft originating in a libration point orbit. Given the limited fuel available for the end-of-life phase, the spacecraft's behavior will be driven by the gravitational influence of solar system bodies. First, we will study whether the CR3BP captures the relevant dynamical behavior observed in an ephemeris model. Then within the framework of the CR3BP, we will consider the role of the unstable manifold for trajectories departing a libration point orbit. These ideas can be used as tools for computing end-of-life probabilities.

In order to study the end-of-life dynamics in an ephemeris model, we must first generate libration point orbits in this model. For the moment, let us consider the L_2 family of Lyapunov orbits. These are periodic orbits in the CR3BP as shown in Figure 2. The ephemeris model, however, is time dependent, and periodic solutions no longer exist. Nevertheless, similar orbits can be generated, which are shown in Figure 4 for one "period" of approximately 6 months, though the orbits do not exactly repeat. We can view these ephemeris solutions as the initial orbits from which end-of-life trajectories will originate.

As a first comparison between the CR3BP and

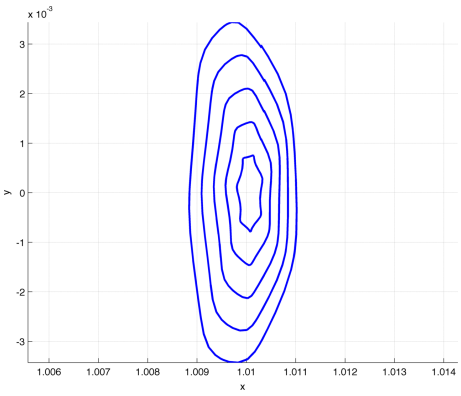

Figure 4: ephemeris Lyapunov orbits

ephemeris dynamics, we perform a Monte Carlo analysis about the reference Lyapunov orbit in each model. For this study, we apply random position perturbations of magnitude 200 km to states along the orbit. As long as the perturbation is sufficiently small, the precise choice of perturbation has little influence on the results. A total of 100,000 trajectories are generated from the set of initial conditions. Due to the influence of the unstable manifold, which will be investigated in this section, half of the trajectories depart towards the Earth, and half depart away from the primaries. Due to the end-of-life restrictions in the Earth vicinity, we will focus on this latter set of exterior trajectories.

In order to classify the outcome, we can check whether the exterior trajectory eventually returns to the Earth vicinity. For the time being, let us define this as being within twice the Moon's radius of the Earth. When the set of exterior Monte Carlo trajectories first depart the libration point orbit, none of the spacecraft trajectories have entered the Earth vicinity. As we consider longer intervals of time, an increasing percentage of the trajectories will have crossed this region at some point along their path. This is illustrated in Figure 5 over a 100-year time period. The first spacecraft returns appear after approximately 15 years. A second set of returns appear between about 25 and 30 years from their libration point orbit departure. This trend is seen in both the CR3BP and ephemeris results. An additional observation is that natural trajectories departing from larger Lyapunov orbits tend to have a higher probability of returning to the Earth. It should also be noted that the ephemeris trajectories considered tend to have a one to two percent higher chance of return within 100 years. This is likely due to the influence of the Moon, which is not included in the Sun–Earth CR3BP, and can be investigated further in the future.

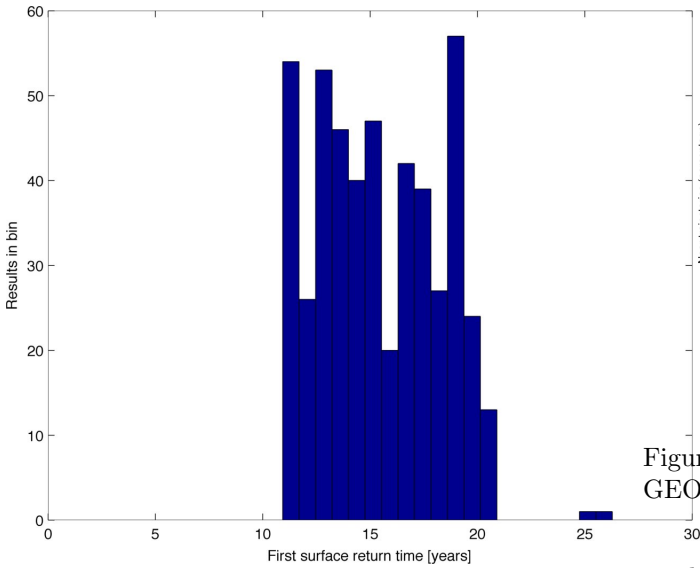

Figure 6: time for revolution about ZVS (halo orbit)

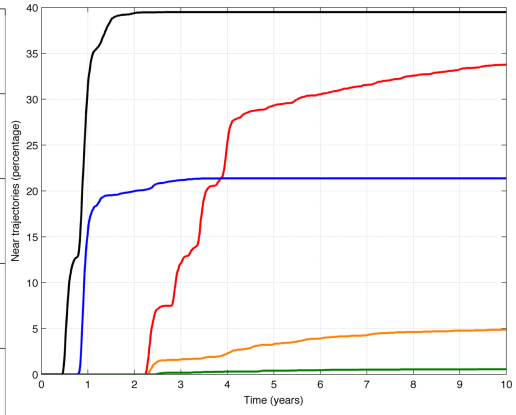

Figure 7: earth vicinity trajectories passing within GEO radius (this is for CR3BP)

Nevertheless, the overall return behavior seen in the CR3BP and ephemeris results is quite similar.

The results can be understood by considering the forbidden regions and zero-velocity surface presented in the previous section. At the Jacobi constant level of the libration point orbits, the forbidden region makes a thin circular shape centered about the Sun with a small opening at the Earth. For an exterior trajectory, the semi-major axis is larger than the Earth's and, thus, has a longer two-body period about the Sun. Therefore, in the rotating frame, the trajectory rotates clockwise while "bouncing" off the the ZVS. Depending on the particular initial conditions, after one revolution the trajectory can either enter through the L_2 gateway or make a subsequent revolution around the ZVS. This is the basis for the jumps seen in Figure 5. If we define a surface at $y = 0$ and include condition $\dot{y} > 0$, we can investigate the time between intersections. This is shown for a representative orbit in Figure 6. This shows the time required for a revolution of the ZVS by non-return trajectories is between 10 and 20 years. Note that similar behavior is observed for interior trajectories departing from an L_1 libration point orbit except that their two-body period is less than the Earth's, and, thus, they rotate counter-clockwise.

The ZVS influences the Earth return results in an additional manner. Larger libration point orbits correspond to Jacobi constant levels with larger gateway openings to the Earth regime. Therefore, a trajectory departing a larger orbit will have a greater probability of returning to the Earth after a revolution about the ZVS. This behavior is observed in Figure 5.

The focus so far has been on trajectories that depart a libration point orbit in a direction away from the Earth. For trajectories directed towards the Earth, as a simple study we consider the same set of L_2 Lyapunov orbits in the CR3BP. We look at their probabilities of passing within the geosynchronous radius over a 10-year interval. In Figure 7 we see that for the larger orbits considered well over 20 percent pass inside this radius within 4 years. While this analysis does not consider the Moon, it emphasizes the potential risk posed by end-of-life trajectories near the Earth.

We have thus far considered the correspondence between the natural motions in the CR3BP and the ephemeris models using a Monte Carlo analysis. However, there is an underlying dynamical structure, namely the unstable manifold, that dominates the motion away from the initial libration point orbit. The benefit of taking advantage of this special structure is that it allows us to easily parameterize states departing the initial orbit using two (for periodic orbits) or three (for quasi-periodic orbits) variables.

In order to numerically generate the manifold, the typical approach (see, for example, [9]) is to determine a linear approximation of the unstable direction relative to the libration point orbit. A small perturbation in this direction is made, and these initial conditions are propagated forwards in time to globalize the manifold. For the Sun–Earth system, scaling the perturbation's position component to about 200 km is a reasonable choice. One important observation is that the sign of this perturbation is free. This allows us to generate two "halves" of the unstable manifold: one departing towards the Earth and one departing away from the Earth. In Figure 8, we show the half of an L_2 orbit's unstable manifold departing away from the Earth. We also show trajectories starting from

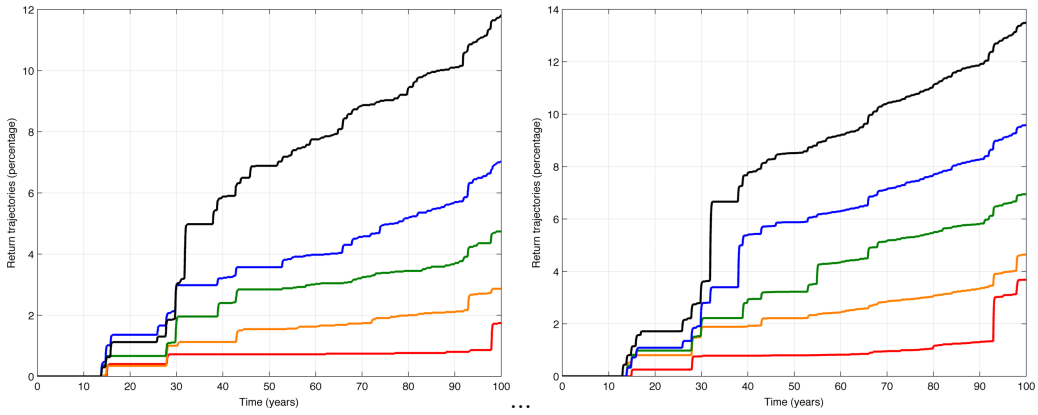

Figure 5: exterior trajectories returning to Earth region (CR3BP left, ephemeris right)–match axes limits

random perturbations on the orbit state. We can see see the underlying influence of the unstable manifold in these results.

An important consequence of the manifold structure is that following solely the natural dynamics, there is a fifty percent chance of heading towards the Earth (which, unless done intentionally, should be avoided), and a fifty percent chance of departing away from the Earth. However, a small maneuver should be possible to switch between the outcomes. The fundamental idea is that the projection of the post-maneuver state onto the unstable subspace should be directed away from the Earth.

An additional benefit of considering the unstable manifold, along with the complementary stable manifold, is that it provides an additional option for locating trajectories that return to the Earth vicinity. Specifically, for planar motion in the CR3BP, the stable manifold serves as a boundary between return and non-return trajectories [10]. Using a suitable surface of section, in this case $y = 0$, $\dot{y} > 0$, we plot in Figure 9 the the closed curves representing the first intersections of an L_2 Lyapunov orbit's stable and unstable manifolds. The segments of the unstable manifold lying in the interior of the stable manifold will return to the Earth after one revolution of the ZVS. The second intersections of the remaining unstable manifold segments can be used to find returns after two revolutions, and so forth. The primary challenge of this approach is that the geometry can become quite complicated. Even for the first intersections shown in Figure 9, the closed curves are distorted into narrow spiral-like shapes. The situation becomes even more complex in the spatial CR3BP where the stable manifold of the center manifold should be considered.

While the direct application of the stable manifold to the computation of returns can be challenging, it still provides an important geometric understanding

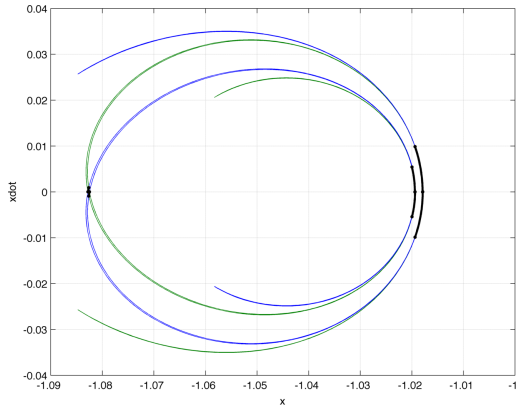

Figure 9: stable (green) and unstable (blue) intersections

of the return behavior. For example, assume that a large number of trajectories on the unstable manifold are generated and return trajectories are located by monitoring the distance from the Earth. The boundaries of the return interval can be be determined using a bisection approach based on the return or non-return outcome. Refinements to this basic scheme can make it more robust, but it suffices to give a first look at intervals on manifold that naturally return to Earth without recourse to a Monte Carlo-style approach. This is used to generate the first return segments shown in Figure 9. Similar ideas could be applied to the study of out-of-plane orbits, but they are not investigated now. However, the behavior should follow a similar trend to the planar orbits since the out-of-plane dynamics are uncoupled to first-order(?).

It is apparent overall that there a close correspondence between the dynamics in an ephemeris model and the CR3BP. In particular, the dynamics are strongly influenced by the unstable manifold, which provides a set of natural end-of-life trajectories. Some

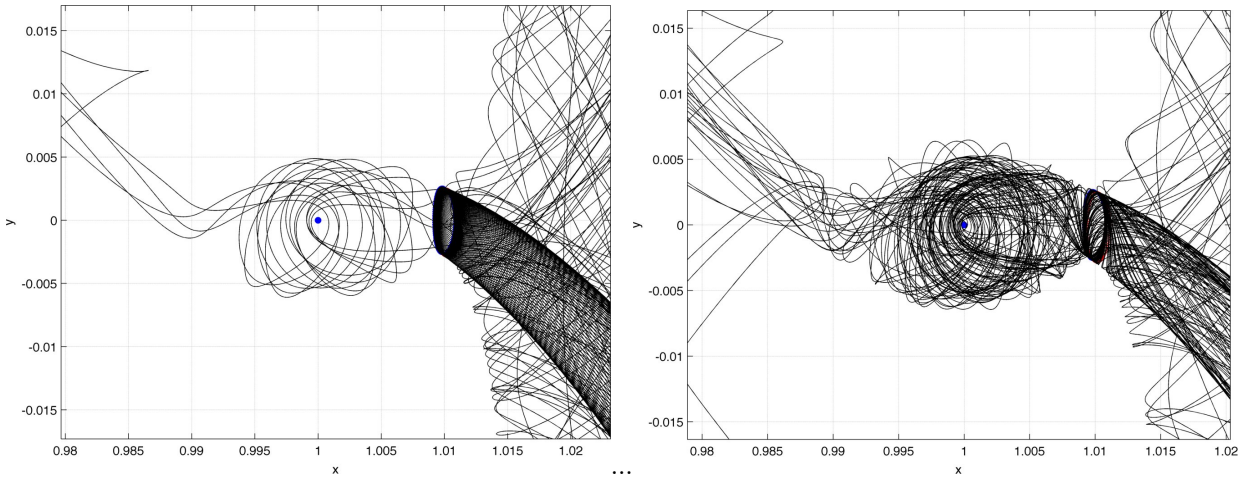

Figure 8: caption

of these trajectories have more desirable outcomes than others. If the probability of a successful disposal is not deemed sufficient, maneuvers can be incorporated to achieve a desired result.

3 Closing zero-velocity surface

In this section, we will consider performing a simple maneuver to forbid a future return to the Earth vicinity. If such a maneuver is possible, the protection requirements for the Earth and its satellite zones would be satisfied. We will analyze the associated maneuver costs and times to determine whether this is a feasible end-of-life scenario. The primary idea will be to take advantage of the dynamical structure, specifically the unstable manifold and the zero-velocity surface (ZVS), present in the CR3BP. It could then be shown that a shadow of this structure persists when a more accurate ephemeris model is considered.

For a spacecraft orbit about the L_1 or L_2 libration points, the corresponding ZVS must be open at that libration point. Otherwise, the orbit would pass through the forbidden region and not be a valid solution. As discussed in the previous section, this mean that trajectories departing the orbit have the possibility of eventually returning to Earth. A maneuver, however, allows us to change the Jacobi constant (or, equivalently, the energy) effectively modifying the geometry of the zero-velocity surface. If the level is changed such that the Earth region and the interior or exterior region are disconnected by a forbidden region, a return to the Earth vicinity for a spacecraft outside it is impossible at least under the CR3BP dynamics. (could discuss earlier ZVC figures)

Prior to performing this maneuver, the unstable manifold will drive the dynamics. In order to separate the spacecraft from the Earth region, we consider the half of the manifold departing away from the Earth towards the interior region for an L_1 spacecraft and towards the exterior region for an L_2 spacecraft. A small correction burn could be used to accomplish this, but this is not currently studied.

For this preliminary analysis as well as in the interest of mission simplicity, once the spacecraft has departed the initial libration point orbit, we consider the most basic option: a single, impulsive maneuver to change the Jacobi constant. Recalling the geometry of the ZVS shown in Figure 1, the surface will first become closed when the Jacobi constant C is increased (energy is decreased) to that of the libration point C_{L_i} $(i = 1, 2)$. Returning to equation (2), for a spacecraft with position and velocity $(\mathbf{r}, \mathbf{v})$, the maneuver $\Delta\mathbf{v}$ must satisfy

$$C_{L_i} = 2U(\mathbf{r}) - \|\mathbf{v} + \Delta\mathbf{v}\|^2. \tag{3}$$

Let us first consider when a solution to this equation exists. If $C_{L_i} > 2U(\mathbf{r})$, there is no possible maneuver to close the gateway to the Earth at this position. Physically, this means that the current position $\mathbf{r}$ lies in the forbidden region associated with Jacobi constant C_{L_i}, and, thus, this is not a appropriate place for a maneuver. Even if a solution exists, certain positions $\mathbf{r}$ correspond to a state in the Earth's region after the maneuver and not in the interior or exterior region. This is an undesirable outcome for an end-of-life disposal trajectory, and these solutions are discarded.

A simple illustration of the geometry is shown in Figure 10. A trajectory departing away from the primaries on the unstable manifold of an L_2 Lyapunov

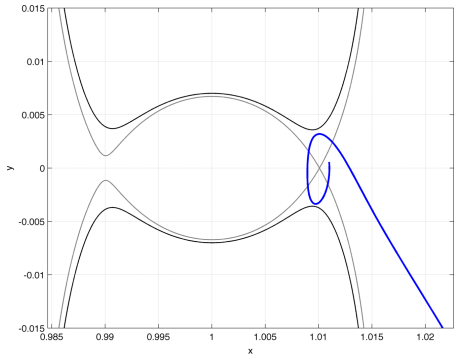

Figure 10: diagram to describe procedure

orbit is shown in blue. The zero-velocity surface at this Jacobi constant level is shown in black, and in gray is the ZVS at the Jacobi constant level C_{L_2} of the libration point. Initially, the position $\mathbf{r}$ is in the exterior region relative to this new ZVS, then passes through the forbidden region, the Earth region, the forbidden region again, and finally out to the exterior region. The end-of-life scheme described can be applied at any point on this trajectory in the exterior region. It is not applicable for the other segments.

Once appropriate positions on the unstable manifold have been identified, the maneuver cost can be calculated. From an inspection of equation (3), it can be observed that most efficient maneuver increasing the Jacobi constant will be in the direction $-\mathbf{v}$. This allows us to compute the cost to be

$$\|\Delta\mathbf{v}\| = \|\mathbf{v}\| - \sqrt{2U(\mathbf{r}) - C_{L_i}}, \tag{4}$$

which is well defined for positions outside of the forbidden region.

Let us now consider the results for various families of initial libration point orbits. In Figure 11, we include maneuver costs for various size L_2 Lyapunov orbits with amplitudes A_y ranging from 100,000 to 600,000 kilometers. Note that the unstable manifolds associated with the periodic orbits we study are two dimensional. For presenting the results we parameterize the manifold as follows. On the vertical axis, an angle uniformly parameterizing the initial periodic orbit in time is used. On the horizontal axis, the time traveling on the unstable manifold is shown. Each trajectory on the unstable manifold, thus, traces out a horizontal line. The coloring corresponds to the cost computed using equation (4) to close the ZVS at that point along the manifold. Uncolored regions correspond to states on the manifold that are either in the Earth or the forbidden region at the new Jacobi constant level.

Examining Figure 11, we see that for each orbit initially there is only a narrow segment that allows the ZVS to be closed and the spacecraft to be trapped in the exterior region. Furthermore, the maneuver Δv along this band are on the order of hundreds of meters per second for the larger Lyapunov orbits considered. Once we pass approximately 6 months on the unstable manifold, however, a maneuver closing the ZVS is possible for all the trajectories. The cost reduces to the order of meters per second.

The cost profile for L_2 halo periodic orbits close to their bifurcation with the Lyapunov orbits follows a similar trend as shown in the upper left of Figure 12. For halo orbits with larger out-of-plane components, however, the initial orbit is completely contained within the forbidden region at the Jacobi constant level C_{L_2}. We need to get a sufficient distance along the unstable manifold away from the initial halo orbit to close the ZVS. Nevertheless, after about 8 months, the scheme can be applied at a cost on the order of X m/s.

Next we consider a Lissajous orbit of amplitude 600,000 km about the L_2 libration point. As before, we can depart this orbit along the unstable manifold and then perform a maneuver to close the zero-velocity surface at the L_2 libration point. However, the manifold is three-dimensional, so we must use three variables to parameterize it. The sequence of images shown in Figure 13 all correspond to a single initial orbit. Each plot uses two angles to parameterize the initial state on the torus from which the manifold trajectory departs (subject to a small perturbation). The sequence is for different amounts of time along the manifold. This allows us to explore the full space of maneuvers for this particular initial Lissajous orbit. Initially, there are just small regions that correspond to potential maneuvers (analogous to the situation with the Lyapunov orbits). These maneuvers have prohibitively high cost. However, the space of potential maneuvers increases as the spacecraft departs along the manifold. Furthermore, the associated cost decreases. At eight months, any trajectory on the manifold has a valid maneuver on the order of tens of meters per second. The cost decreases from there to the order of meters per second. (can also include 100,000 km Liss images)

For illustrative purposes, as a modification of the current scheme, we consider the half of the unstable manifold heading towards the Earth. In this case, we can consider trajectories that pass through the bottleneck and into the interior region. A maneuver can then be performed to trap the spacecraft in this region away from the Earth. The results for a 400,000-km Lyapunov orbit are shown in Figure 14. The sit-

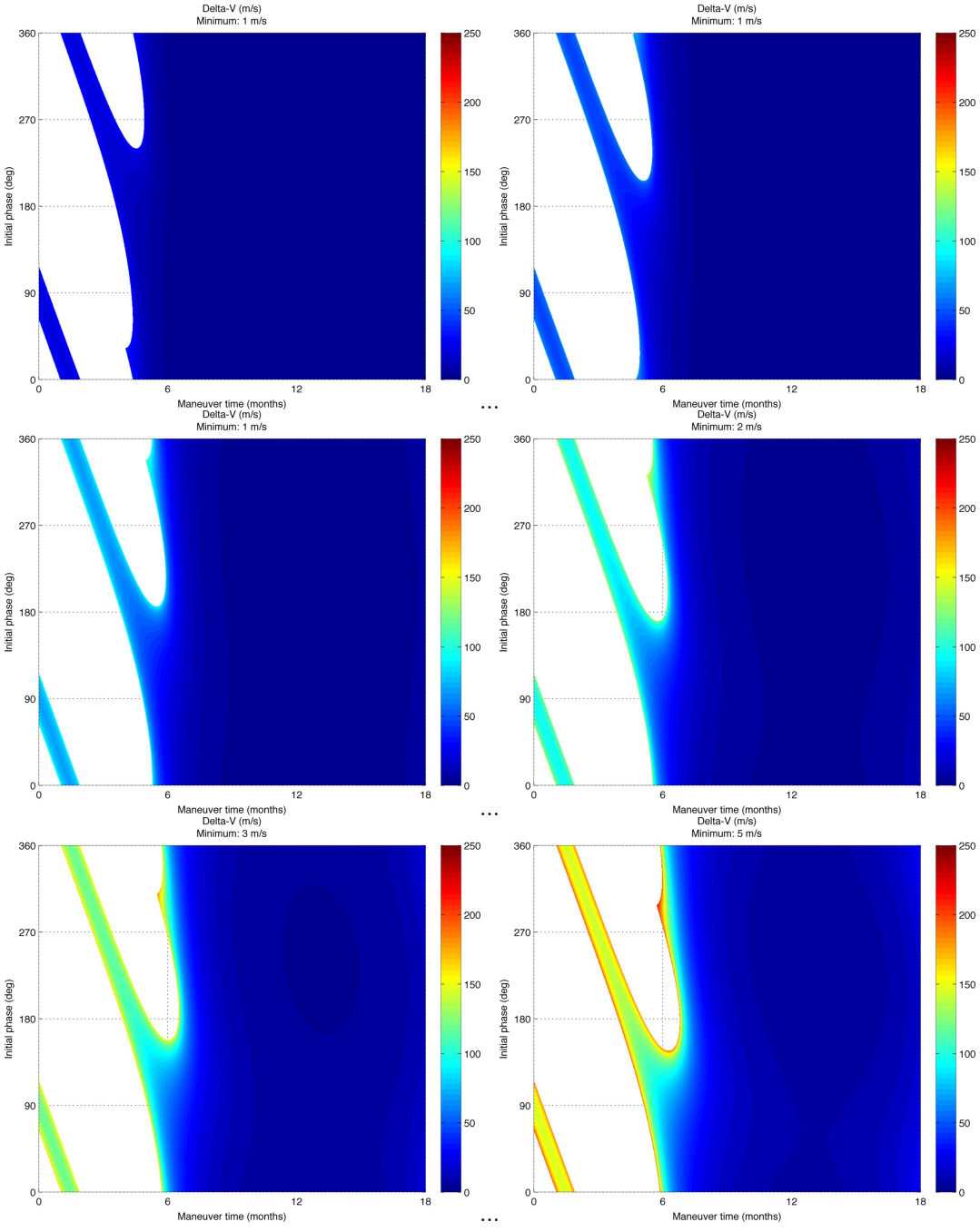

(and more)

Figure 11: Lyapunov costs

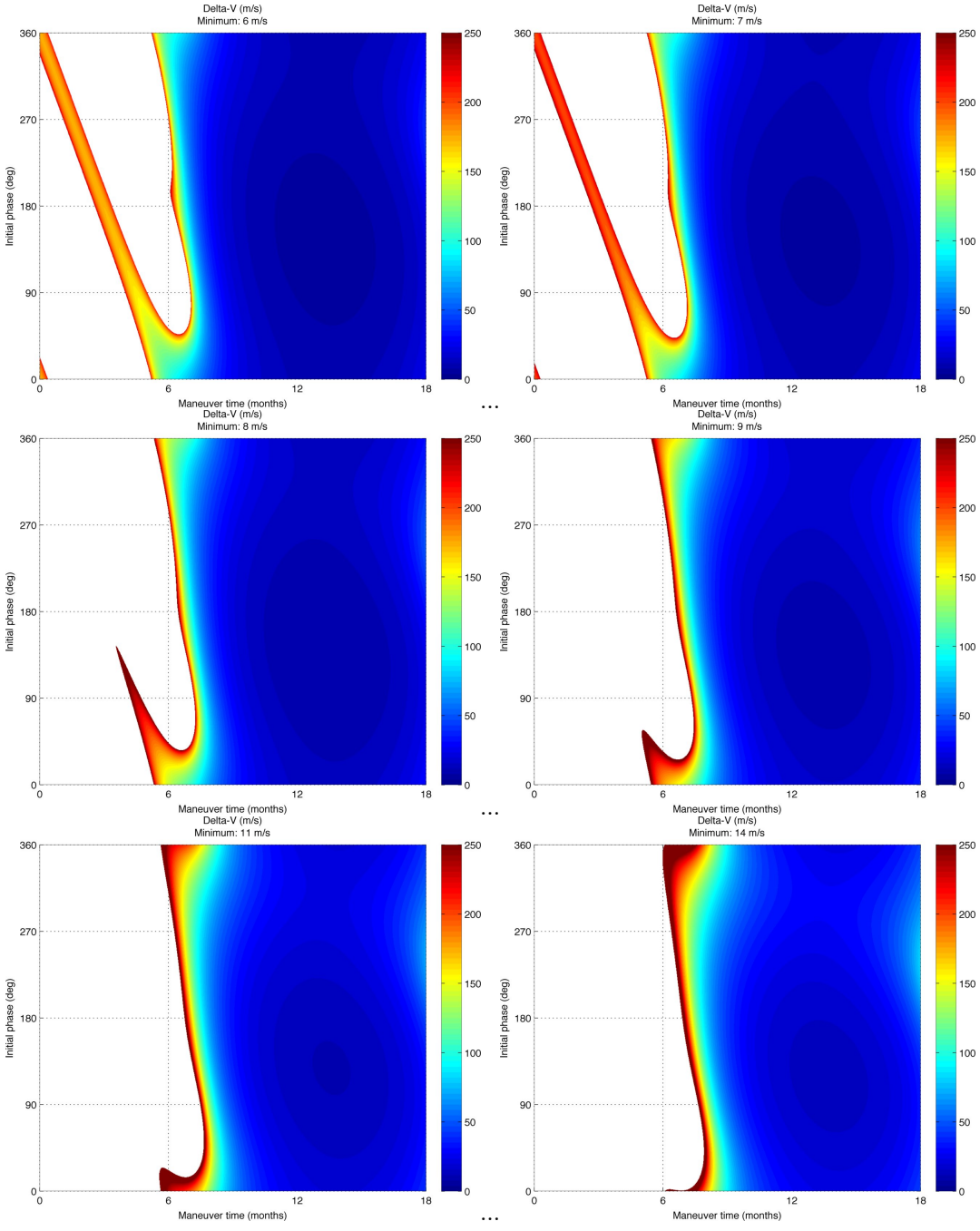

(and more)

Figure 12: L_2 halo costs

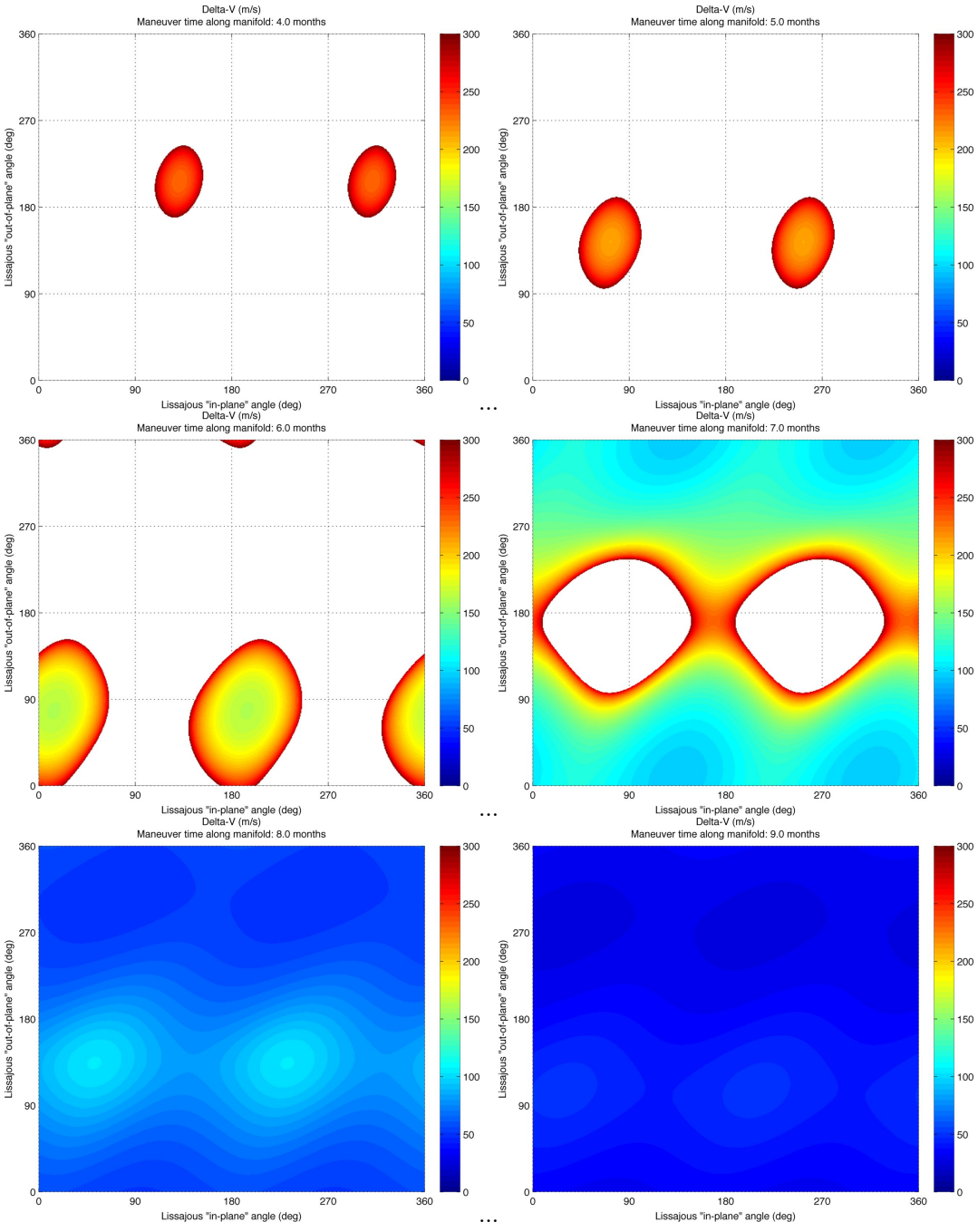

(and more)

Figure 13: L_2 600,000-km Lissajous

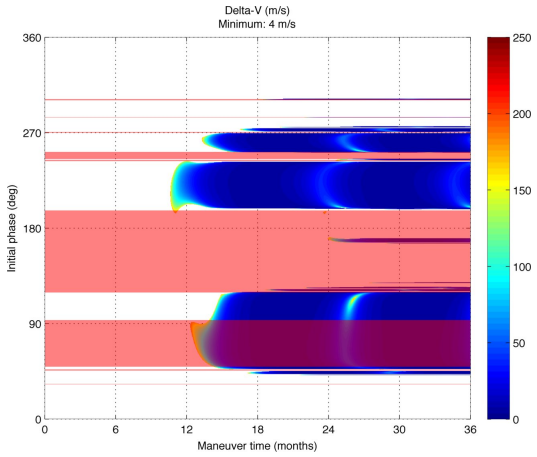

Figure 14: passing by Earth, 400,000-km Lyapunov (note: Moon will influence true behavior)

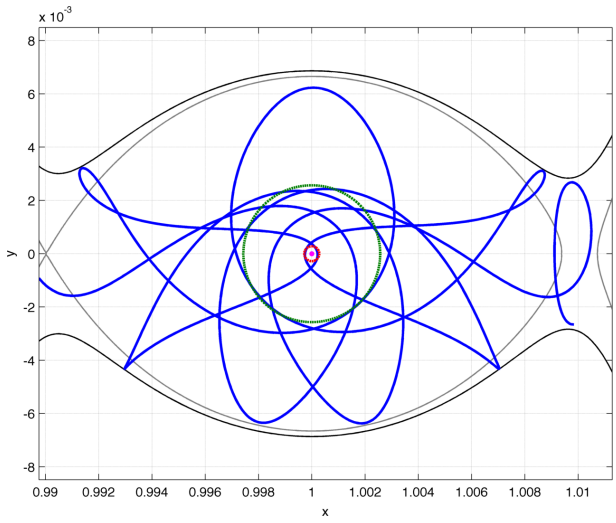

Figure 15: geometry of Moon collision

uation is much more complex in this region. Only certain segments on the manifold satisfy the necessary conditions and the maneuver time is at least one year after departing the initial orbit. In red highlight, trajectories passing within the geosynchronous radius are shown, which could lead to additional end-of-life constraints. Furthermore, the Moon's influence is not included, which could significantly affect these transit trajectories. This example emphasizes the simplicity gained by considering exterior trajectories rather than interior trajectories subject to chaotic dynamics.

(put in discussion for ephemeris computation)

4 Terminal solutions

In order to permanently dispose of a libration point spacecraft, it must be brought to a solar system body. In the context of this analysis, the most direct options are the Sun, Earth, and Moon. The control required to impact any other body such as an asteroid would fit more as a follow-on mission and is beyond the scope of the current study. In this section, we discuss the general aspects of the terminal outcomes. More detailed study would be possible in later work.

Since a spacecraft in an L_1 or L_2 libration point orbit is approximately in a circular orbit relative to the Sun, a disposal into the Sun would require the semi-major axis to be roughly halved. This would require a significant change in energy, and this will likely exceed the amount of fuel available to the spacecraft. Using a sequence of flybys, etc. could reduce this cost, but again is beyond the current scope and would require end-of-life planning effort well beyond a typical mission.

As a second possibility, there is the option of an Earth collision orbit. However, there are logistical issues associated with this. First, precise control would be necessary to target the Earth. Second, it would necessarily pass through protected orbital regions, which would require careful planning dealing with uncertainties. Third, a spacecraft reentering the atmosphere will break-up and needs to have safe disposal site such as into ocean. This option is not considered in general for the constraints listed in the first section, but specific analysis for a particular mission could be performed to assess feasibility.

The final disposal option to consider is a collision into the Moon. As opposed to an Earth collision orbit, a Moon collision orbit would be subject to fewer restrictions. Furthermore, the unstable manifold from libration point orbits often cross the orbit of the Moon. In Figure 15, a trajectory departing towards the Earth on the unstable manifold of an L_2 Lyapunov orbit is shown. It has many crossings with the Moon's orbit shown in green. A collision with the Moon, however, would require the Moon to have an appropriate phase in its orbit. This would require precise planning and targeting, which may introduce additional complexity into the end-of-life planning scheme, but the potential for a completely final outcome warrants future consideration. Preliminary analysis shows a single maneuver of cost less than 100 m/s is possible for several possible phasings.

5 Concluding remarks

This study provides a first look at the dynamics applicable to the end-of-life disposal for libration point spacecraft. The primary constraints relevant to these

spacecraft are the avoidance of space debris (planetary protection) and limiting the fuel, time, and complexity of this mission phase. This leads to the consideration of natural motions in both an ephemeris and CR3BP model and associated outcome probabilities. It is apparent that the unstable manifold is the primary driver of motion away from the orbit. Using a small maneuver, it should be possible to place a spacecraft on an unstable manifold external trajectory away from the L_2 libration point (or an internal trajectory away from the L_1 libration point) avoiding the Earth bottleneck regime. By including an additional maneuver on the unstable manifold, the bottleneck can be closed. This was seen to have a relatively low cost though the maneuver must be performed after about 6 months. Assuming that this time period is acceptable, this seems like a simple option to dispose of a libration point spacecraft. Comments were also made about the possibility of a terminal disposal option primarily into the Moon.

There are many directions for future investigation. More complicated maneuver schemes could reduce the time required to close the zero-velocity curve, which may be a worthwhile tradeoff for additional fuel use and complexity. In a context of a particular mission, more detailed analysis could be conducted and aspects such as the ephemeris epoch could be set accordingly. In addition, each mission has its own unique set of constraints that must be balanced. In certain cases, the terminal options may warrant further consideration. Further analysis of internal trajectories inside the Earth's orbit from the L_1 libration point would be insightful. Analysis of the influence of inaccuracies in the thrust magnitude and direction could also be studied statistically.

Acknowledgements

The authors would like to acknowledge support from Marie Curie Research Training Network AstroNet-II. In addition, the first author is grateful for support from the International Astronautical Federation to attend the conference through the Emerging Space Leaders Grant Programme.

References

[1] iso-24113 space debris mitigation requirements

[2] ISEE-3 mission and Earth passage

[3] SOHO trajectory design

[4] HERSCHEL and PLANCK end-of-life

[5] future libration point missions

[6] Roy, Orbital Motion

[7] NASA JPL DE422

[8] Bulirsch–Stoer algorithm, ODEX

[9] generating manifold - dynamics and mission design near libration points?

[10] Gomez et al., Connecting orbits and invariant manifolds in the spatial restricted three-body problem (verify, or maybe use a periapsis map paper(?))